

OPTICAL FIBRES

https://doi.org/10.1070/QEL16962

Optimal design of a single-mode trench-assisted homogeneous multicore fibre with a minimum crosstalk level

Dablu Kumar, Rakesh Ranjan

Abstract. **We have proposed an optimal design of five different core structures (St1–St5) for a seven-core trench-assisted multicore fibre, whose core radius and relative core/cladding refractive index difference Δ_1 are optimal for single-mode propagation. The crosstalk performance and its reduction (in dB) with respect to variations in fibre design parameters, such as cladding/trench (Δ_2) depth and trench width W_t are investigated. It is shown that some fibre operational parameters, like, fibre bending radius, operating wavelength and fibre length, affect the crosstalk performance. It is found that the crosstalk and its reduction amount are extremely dependent on the values of Δ_1 and Δ_2. The dispersion characteristics of the cores are investigated for all the proposed core structures and the observed dispersion is found to be about –6 ps nm^{-1} km^{-1} at an operating wavelength of 1550 nm. An ultralow crosstalk (less than –100 dB per 100 km) can be achieved mainly with two proposed core structures (St4 and St5) having a suitably higher values of Δ_1 along with a small core radius for single-mode propagation. The multicore fibre design with many cores (up to 55) is demonstrated to ensure a high transmission capacity.**

Keywords: *multicore fibre, refractive index profile, trench-assisted core, crosstalk, crosstalk reduction amount, large number of fibre cores.*

1. Introduction

Space division multiplexing based multi-core fibre (MCF) is one of the most suitable candidates to meet the exponentially increasing demand of data transmission capacity, which increases 100 times every ten years. In conventional single-core single mode fibre (SC SMF), the transmission capacity is mostly limited to around 100 Tbit s^{-1} [1]. An increase in the core diameter makes it possible to pass more modes, which improves the transmission capacity, but simultaneously, causes the interference of modes with each other. MCF, not only improves the capacity/bandwidth of the optical fibre technology [2–4], but also largely reduces the mode interference. In order to achieve the enhanced capacity, the specific design and analysis of MCF must be taken into consideration before the fabrication process, because the presence of more than one core in a single cladding region may cause the phenomena of crosstalk (XT) between the cores [5], known as inter-core crosstalk (ICXT). Based on coupling phenomena, MCF can be categorised into strongly coupled and weakly coupled MCFs [6]. For weakly coupled MCF, the ICXT is one of the major hurdles for the propagation of the optical signal, which proportionally increases with transmission distance. Therefore, the XT reduction in MCF is one of the main concerns for long-haul high capacity optical fibre communication. Nevertheless, with a suitable design, the ICXT in MCF can be restrained within a certain limit (such as $<$ –30 dB per 100 km) [7]. Normally, to achieve the XT of –30 dB, the mode-coupling coefficient between the two neighbouring cores must be less than 10^{-2} per meter [6] for a transmission distance of ten kilometres or more by losing the spatial density with a core pitch of around 40 μm or more.

Recently, the XT reduction in MCF has been one of the main concerns for long-haul high capacity optical fibre communication. There are several methodologies proposed for the reduction of crosstalk, such as trench-assisted (TA) technique [8, 9], heterogeneous core method [6] and propagation direction interleaving approach [6, 10], etc. Many researchers over the world are working in the area of multicore fibre [5–8, 10–14] for crosstalk performance analysis. Some of the recent developments in this research area have been described in [9, 15–24], and simultaneously, work based on MCF characterisation and its applications have been reported in papers [25–34]. In [8, 10], the XT reduction in a homogeneous MCF has been presented by utilising the approximate method. The analytical expression for crosstalk reduction (ΔXT) in a TA MCF structure with respect to the normal step-index core has been derived. The authors of Ref [10] have analysed the crosstalk reduction amount using the approximate method in terms of the trench width ratio ($R_{tr} = W_t/x_1$) and the ratio of relative refractive index differences ($m = |\Delta_2|/\Delta_1$) between two neighbouring cores in MCF, based on the parameters provided in Table 1 [10]. The results from Ref. [10] have been re-simulated and validated using the approximate method as well as the semi-analytical method, which is consisting of the finite element method (FEM) based simulation and analytical computations.

In the current paper, the results of work [10] have been extended to examine the behaviour of crosstalk and its suppression in terms of various fibre designs and fibre operational parameters, such as the relative core/cladding refractive index difference Δ_1, cladding/trench depth Δ_2, trench width W_t, wavelength, transmission distance and bending radius by using the semi-analytical approach for the five newly proposed core structures. The authors of [10] have only analysed XT and ΔXT in terms of some wavelength range and the ratio of relative refractive index differences respectively,

Dablu Kumar, Rakesh Ranjan Optical Fibre Communication and Photonics Lab, Department of Electronics and Communication Engineering, National Institute of Technology (NIT) Patna, Patna-800005, India; e-mail: dablu.ece15@nitp.ac.in

Received 6 February 2019; revision received 3 August 2019
Kvantovaya Elektronika **49** (11) 1045–1053 (2019)
Submitted in English

while other significant parameters have not been addressed. Therefore, new analysis has been extended for the exactly same core structure as provided in Table 1 of [10] in terms of all the above-mentioned fibre parameters and these newly derived results have been compared with the simulated results for all the five proposed core structures. This comparison enables us to search for an optimal core structure design in order to achieve ultralow crosstalk levels in MCF. The core structure parameters as shown in Table 1 of Ref. [10] are denoted by 'St0' [10] in this paper. All the five core structures have been designed with different combinations of core radii x_1 and the Δ_1 values, strictly for the single-mode propagation condition with a cutoff wavelength of nearly 1520 nm, in order to analyse the crosstalk performance for a 7-core MCF [13]. The coupled mode theory (CMT) and coupled power theory (CPT) [5, 12] have been used to evaluate the coupling coefficient [33] and hence, the ICXT in MCFs, considering the bending effects [11, 27]. It has been verified that the results of the semi-analytical approach are very similar to that of the approximate analytical method. The impact of the number of interfering cores (single or multiple) on the mean ICXT power level is discussed. The dispersion characteristic is inspected by varying the wavelength to ensure that the designed MCF core structures have significantly low dispersion values (less than -5 ps nm^{-1} km^{-1}), at an operating wavelength of 1550 nm for single-mode propagation.

The paper is organised as follows. Section 2 describes the design of optimal core structures (St1–St5) and their effective parameter values. Section 3 presents the methodologies for crosstalk estimation and reduction; here, a new expression for crosstalk under bending and twisting conditions is derived using the conventional method. In Section 4, the dispersion characteristics are discussed for all the proposed five-core structures. The results of XT performance and its reduction in terms of various fibre designs and fibre operational parameters are presented in Section 5. Section 6 presents a discussion regarding MCFs with a preferable core structure for short reach applications and for long-haul communication. This section also described the problem of the implementation of multicore (up to 55) MCF structures to improve the data transmission capacity. Section 7 concludes the results of the work.

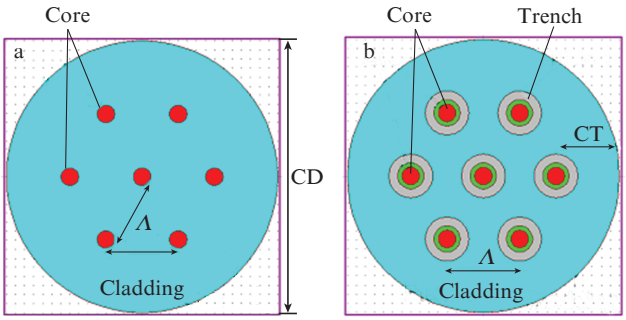

Figure 1. (a) Seven-core uncoupled homogeneous MCF with a core pitch $\Lambda = 40$ μm and (b) its corresponding TA MCF structure.

2. Proposed multicore fibre designs

Figures 1a shows a 7-core uncoupled homogeneous step-index MCF with six cores in the outer ring of radius of 40 μm and one core at the centre. Figure 1b presents a similar trench-assisted MCF structure. Five different MCF structure designs along with corresponding TA structures have been proposed for single-mode propagation by varying the core radius from 3 to 5 μm, with the corresponding variations in Δ_1 as depicted in Table 1. These Δ_1 values have been chosen optimally corresponding to each of core radius values after simulating these core structures several times under the constraints of single-mode propagation through the fibre cores, whereas, the authors of paper [10] have considered the generalised value of Δ_1 (0.35%), instead of its optimal value.

The main motivation for the current work is to search for the optimum core structure for the ultralow crosstalk behaviours under single-mode operation. The TA approach [6, 9] is one of the important methods to reduce the coupling (hence, the ICXT between two adjacent cores) to a significantly low level by incorporating a trench around the cores in MCF structures. The trench is a boundary structure having a refractive index profile lower than that of the core and cladding.

The refractive index profiles for a step index core and TA step-index core MCF are shown in Fig. 2, where x_1 is the core radius, and x_2 and x_3 are, respectively, the distances from the centre of the core to the inner and outer border of the trench with $x_2 = 2x_1$. The trench width W_t is assumed to be equal to 5 μm for all five proposed core structures, while, for St0 it is 4.5 μm [10]. The refractive index of the core region, n_1, is the same for both normal and TA step-index cores, n_2 is the refractive index of the trench and $n_0 = 1.45$ is the refractive index of the cladding region. The relative core/cladding refractive index difference is Δ_1, and the cladding/trench refractive index difference is Δ_2. The distance between any two neighbouring cores, (i.e., core pitch Λ), should be such

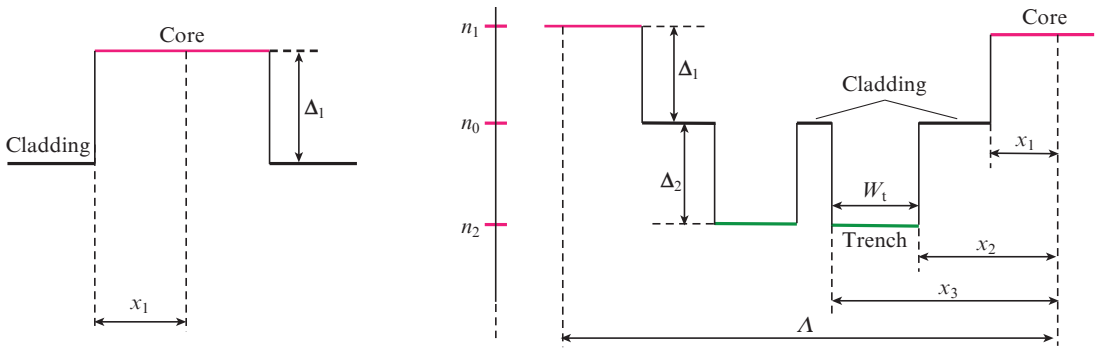

Figure 2. Refractive index profile of (left) a step-index core and (right) a TA step-index core [14].

Table 1. Design parameters of homogeneous multicore fibre.

Parameter	St0 [10]	St1	St2	St3	St4	St5
Core radius x_1/μm	4.5	5.0	4.5	4.0	3.5	3.0
Cladding diameter (CD)/μm	125	125	125	125	125	125
Cire refractive index n_1	1.4551	1.4558	1.4559	1.4575	1.4598	1.4632
Cladding refractive index n_0	1.45	1.45	1.45	1.45	1.45	1.45
Relative core/cladding refractive index difference Δ_1 (%)	0.35	0.33	0.40	0.51	0.67	0.90
Effective refractive index n_{eff}	1.452454	1.452451	1.453115	1.453921	1.455188	1.456957
Effective mode area A_{eff} /μm^2	93.6	75.8	59.7	45.6	34	
Cutoff wavelength λ_c/nm	1517	1514	1517	1518	1511	
n_{eff} of a TA core at $\Delta_2 = -0.70\%$	1.452519	1.453089	1.453892	1.455157	1.456921	
n_{eff} of a TA core at $\Delta_2 = -1.40\%$	1.452512	1.453081	1.453882	1.455144	1.456904	

that each core in the MCF behaves as a separate spatial channel. The fibre length L, core pitch Λ and operating wavelength λ are set equal to 100 km, 40 μm and 1550 nm, respectively. The detailed design specifications and mode effective parameters are provided below in Table 1.

3. Inter-core crosstalk analysis

The crosstalk (XT) can be defined as the interference caused by the magnetic/electric fields of the signal in one core to the signal of adjacent cores. Due to the presence of many closely packed cores in the same cladding region, the crosstalk between the neighbouring cores is a crucial factor. The XT between the adjacent cores can be quantified in terms of optical signal power, as some amount of optical power propagating through one of the core is coupled with its neighbouring cores during its transmission (Fig. 3). The ICXT between two adjacent cores can be expressed as XT (dB) = $10\lg(P'/P)$, where P and P' are the output optical powers from the input core q and the neighboring core p, respectively [9].

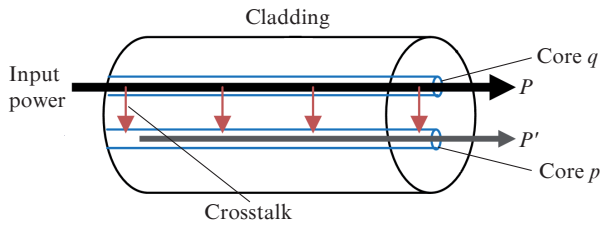

Figure 3. Power coupling from the input core to the neighbouring core [9].

The crosstalk behaviour was analysed using the semi-analytical method, in which the value of the mode propagation constant β in a particular core is first obtained using the FEM based simulation analysis, and then this β value is used in the implementation of CMT/CPT method for the XT assessment. The coupled mode theory (CMT) is a powerful perturbation method for analysis of coupling effects between the adjacent cores in optical fibre. If two cores are adequately close to each other, then the propagating modes in each core may interfere/couple with each other. However, if the distributions of the electromagnetic (EM) field in these cores after coupling weakly differ from those before coupling, the coupled cores can be analysed through the CMT approach. The conventional coupled-mode equations (CMEs) can be expressed as [12]

$$\frac{\mathrm{d}A_p}{\mathrm{d}z} = -\mathrm{j}\sum_{p\neq q} k_{pq}A_q(z)\exp(\mathrm{j}\Delta\beta_{pq}z)f(z), \tag{1}$$

where A_p and A_q are the amplitudes of the mode in cores p and q, respectively; $\Delta\beta_{pq} = \beta_p - \beta_q = -\Delta\beta_{qp}$ is the difference of mode propagation constants between cores p and q; z is the coordinate of the propagation direction; and

$$f(z) = \exp[\mathrm{j}(\Phi_p - \Phi_q)]\delta f(z) \tag{2}$$

is a random phase function accounting for the twisting and bending effects changing the optical length of optical fibre. Here, the first part, $\exp[\mathrm{j}(\Phi_p - \Phi_q)]$ is essentially deterministic, while the second part, $\delta f(z)$ is a stationary random process; and Φ_p and Φ_q are the field phases present in cores p and q caused by bending and twisting. The mode coupling coefficient (MCC) k_{pq} can be expressed as [35]

$$k_{pq} = \frac{\sqrt{\Delta_1}}{x_1}\frac{U_1^2}{V_1^3 K_1^2(W_1)}\sqrt{\frac{\pi x_1}{W_1\Lambda}}\exp\left(-\frac{W_1}{x_1}\Lambda\right), \tag{3}$$

where $W_1 = x_1(\beta^2 - k^2n_0^2)^{1/2}$; $U_1 = x_1(k^2n_1^2 - \beta^2)^{1/2}$; $\beta = kn_{\text{eff}}$ is the mode propagation constant; $k = 2\pi/\lambda$ is the wave number; λ is the light wavelength in vacuum; $V_1 = 2\pi x_1 n_1(2|\Delta_1|)^{1/2}/\lambda$ is the normalised frequency; and $K_1(W_1)$ is the first-order second-kind modified Bessel function.

Another approach, the coupled power theory (CPT), is totally based on the principle of signal power measurement, where the power launched in one of the cores is transferred to its adjacent cores. Compared to CMT, the CPT allows for a more accurate and faster estimation [12] of the average crosstalk in MCFs, where it takes into account the averaged contribution of twisting and bending effects [11]. The coupled-power equation (CPE) can be written as [12]

$$\frac{\mathrm{d}P_p}{\mathrm{d}z} = \sum_{p\neq q} h_{pq}(z)[P_q(z) - P_p(z)], \tag{4}$$

where P_p and P_q are the average powers in cores p and q, respectively; and h_{pq} is the power coupling coefficient (PCC) between cores p and q. When the CPE is solved in simplest form, the expression of the PCC can be realised in terms of MCC as [6]

$$h_{pq} = \frac{2k_{pq}^2 R_b}{\beta\Lambda}, \tag{5}$$

where R_b is the bending radius. Therefore, the final expression for the average crosstalk XT_μ between two adjacent cores in MCF can be written as [5]

$$XT_\mu \simeq h_{pq} L \simeq \frac{2k_{pq}^2 R_b}{\beta\Lambda} L. \tag{6}$$

Equation (6) describes the direct dependence of the average crosstalk on the mode coupling coefficient, fibre bending radius, fibre length and core pitch along with its indirect dependence on the wavelength and effective refractive index. It mostly takes into account the impact of the fibre bending conditions. Moreover, in order to consider the effect of twisting along with the bending conditions, a new expression for h_{pq} is derived using the coefficient of discrete changes K_{pq} [5]. The coefficient of discrete changes caused by the coupling from the core q to the core p can be expressed as [5]

$$K_{pq} \simeq \sqrt{\frac{k_{pq}^2 R_b}{\beta\Lambda}\frac{2\pi}{\gamma}} \exp\left[-j\left(\frac{\beta\Lambda}{\gamma R_b} - \frac{\pi}{4}\right)\right], \tag{7}$$

where γ is the twist rate of fibre [24]. Using the simulation analysis, we found that $h_{pq} \simeq |K_{pq}|^2$. Therefore, the new expression for the crosstalk under the bending and twisting conditions can be simplified as [34]

$$XT_\mu \simeq h_{pq} L \simeq \frac{2k_{pq}^2 R_b}{\beta\Lambda}\frac{\pi}{\gamma} \exp\left[-j\left(\frac{2\beta\Lambda}{\gamma R_b} - \frac{\pi}{2}\right)\right] L. \tag{8}$$

Essentially, Eqn (6) is a special case of Eqn (8) under the twist rate of $\gamma = \pi$ rad m^{-1}, where the exponential term has negligible effect on the XT value. In trench-assisted MCFs, the mode coupling coefficient for two adjacent cores can be expressed as [8, 10]

$$k'_{pq} = \frac{\sqrt{\Gamma}\sqrt{\Delta_1}}{x_1} x_1 \frac{U_1^2}{V_1^3 K_1^2(W_1)} \sqrt{\frac{\pi x_1}{W_1\Lambda}} \times \exp\left(-\frac{W_1\Lambda + 2(W_2 - W_1)W_t}{x_1}\right), \tag{9}$$

where $W_2 = (V_2^2 + W_1^2)^{1/2}$; $V_2 = 2\pi x_1 n_0 (2|\Delta_2|)^{1/2}$; $\Gamma = W_1/[W_1 + (W_2 - W_1)W_t/\Lambda]$; other parameters being the same as above. In the presence of more than one surrounding core, the average crosstalk is estimated numerically as the total sum of ICXT on a specific core by its all-neighbouring cores.

Then, the crosstalk reduction amount ΔXT (in dB), due to the implementation of the trench-assisted core as compared to the normal step index core, can be expressed as [8]

$$\Delta XT \simeq 17.4(W_2 - W_1)\frac{W_t}{x_1} - 10\lg\Gamma, \tag{10}$$

where W_1 can be approximated by $1.1428V_1 - 0.996$ at $0 < \Gamma < 1$.

4. Dispersion analysis

While propagating the signal through the MCF, the pulse broadening, also known as dispersion, is another major hurdle along with the crosstalk. In designing the core, which satisfies the single-mode propagation condition, the dispersion must be in a tolerable range (below 21 ps nm^{-1} km^{-1}) [20]. The results of a generalised analysis of dispersion are shown in Fig. 4 for a particular core with fundamental (LP_{01}) mode propagation. The dispersion $D(\lambda)$ is proportional to the second derivative of the effective refractive index n_{eff} with respect to the wavelength [9, 23], and usually defined as:

$$D(\lambda) = -\frac{\lambda}{c}\frac{d^2 \mathrm{Re}\, n_{eff}}{d\lambda^2} \text{ (ps nm}^{-1}\text{ km}^{-1}\text{)}, \tag{11}$$

where c is the velocity of light in vacuum, and $\mathrm{Re}\, n_{eff}$ is the real part of the effective refractive index. One can see from Fig. 4 that the dispersion impact is very small for all the respective core structures, with less than -6 ps nm^{-1} km^{-1} at $\lambda = 1550$ nm.

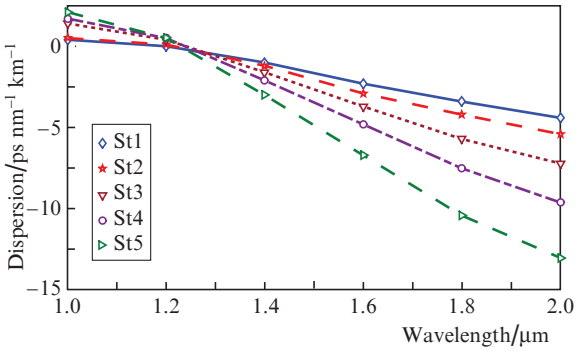

Figure 4. Dispersion vs. wavelength for the five core structures on the example of the LP_{01} mode.

5. Numerical simulation results

The ICXT performance was analysed for all the five presented core structures with respect to the fibre design parameters (Δ_1, Δ_2, W_t) and the fibre operational parameters (R_b, λ, L) in trench-assisted MCFs. By using the FEM-based simulation, the effective refractive index was estimated, which is used for the analytical computation of XT under various fibre-related constraints as mentioned in Section 2 for both normal step-index and TA step-index MCF structures. Further, the obtained results for the proposed core structures were compared with the newly simulated results based on the design of core structure St0 [10] with $x_1 = 4.5$ μm and $\Delta_1 = 0.35\%$, in terms of the above mentioned fibre design and operational parameters.

5.1. Crosstalk vs. relative refractive index difference Δ_1

Usually, the core diameter for the single-mode propagation is from 6 to 10 μm. Figure 5 demonstrates the relation between $\mathrm{Re}\, n_{eff}$ and Δ_1 for the same range of core diameters. One can see that the $\mathrm{Re}\, n_{eff}$ increases gradually with Δ_1, while the imaginary n_{eff} is nearly zero. A small increase in the core diameter can considerably increase the n_{eff} values, which subsequently results in a considerable reduction of the crosstalk level. The estimated values of n_{eff} are further used to calculate the actual XT levels and the XT reduction amount (dB) in TA MCFs (Figs 6 and 7). From the results, it evident that the

XT reduction amount is highly reliant on Δ_1, such as, for its lower values, the XT reduction is quite significant, but at the same time, the mode confinement in cores is low [15], which corresponds to higher XT levels. Hence, the value of Δ_1 must be chosen very precisely in order to take into account both the factors of mode confinement and XT reduction. For example, at the core diameter $2x_1 = 9$ μm and $\Delta_1 > 0.40\%$, the higher order modes propagate further through the MCF cores, which worsens the XT behaviour. Hence, $\Delta_1 = 0.40\%$ is the optimum value for a core diameter of 9 μm. Similarly, for all the other considered core diameters, the optimal values of Δ_1 have been chosen and listed in Table 1, so that only the fundamental mode can propagate through the cores, without introducing any higher order modes.

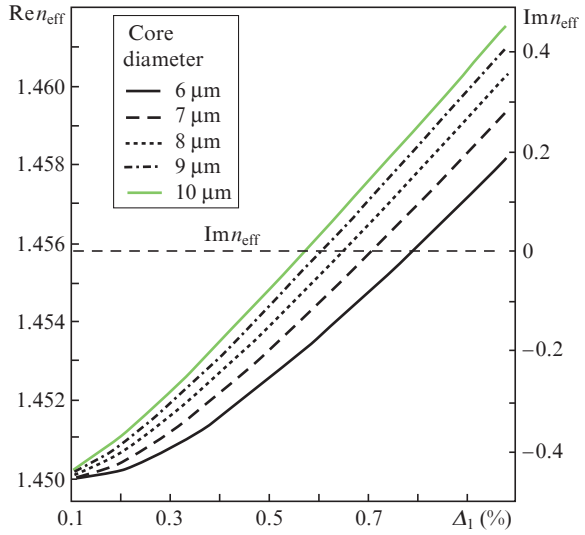

Figure 5. Dependences of Ren_{eff} on Δ_1 at different core diameters.

The results obtained for all the five proposed core structures were compared with the newly simulated results for the core structure St0 [10] ($W_t = x_1$) under the same fibre parameters, such as bending radius, fibre length, core pitch, wavelength, etc. to assess the ICXT value in a particular core. One can see from Fig. 6 that St1 ($2x_1 = 10$ μm) and St2 ($2x_1 =$ 9 μm) have better crosstalk performance in comparison to the core structure St0 [10], while St3 to St5 have comparatively inferior performance, which is mainly due to a smaller core radius at fixed values of Δ_1. As discussed in [10] and also validated in Fig. 7, the performance of the FEM-based semi-analytical approach is very similar to that of the approximate method; therefore, in this paper, the crosstalk behaviour for all the proposed core structures was analysed using the semi-analytical approach only.

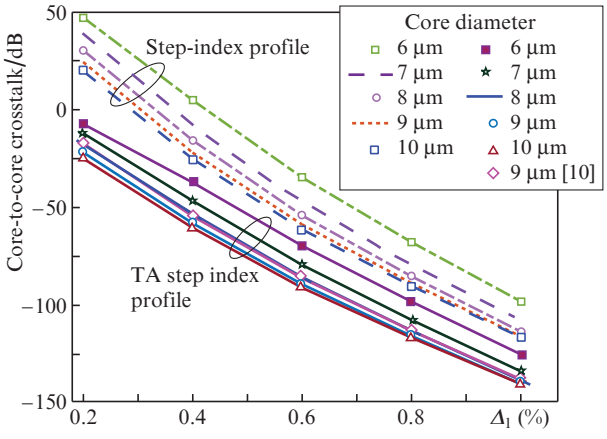

Figure 6. Dependences of the core-to-core crosstalk on Δ_1 at $\Lambda = 40$ μm and $W_t = 5$ μm.

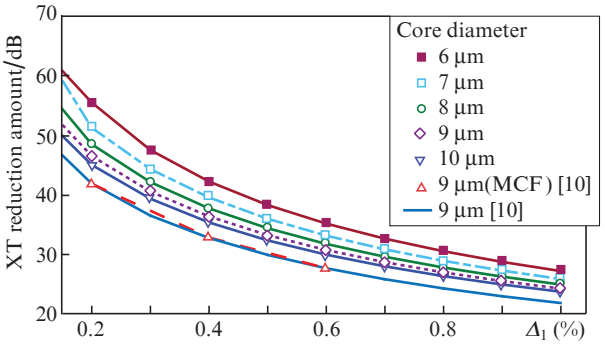

Figure 7. Dependences of the XT reduction amount on Δ_1 at $\Lambda = 40$ μm and $W_t = 5$ μm.

5.2. Crosstalk vs. trench depth Δ_2

Figures 8 and 9 show the results of an analogous XT and XT reduction analysis with respect to trench depth Δ_2 for all the presented core structures at a propagation wavelength of 1550 nm, a bending radius of 140 mm and a core pitch of 40 μm. Figure 9 clearly demonstrates that the higher crosstalk reduction can be achieved with a higher core diameter and higher Δ_2 values, which is mainly because of the fact that a deeper trench depth leads to stronger mode confinement and, henceforth, it lessens the mode overlap between the two neighbouring cores. Simultaneously, the selection of lower Δ_1 (such as St1) may cause a high crosstalk level, as shown in Fig. 8. Therefore, with a suitable choice of higher values of Δ_1 and Δ_2, the ultralow XT levels can be achieved between the neighbouring cores of the MCF. One can see from Fig. 8 that the crosstalk performance of all the five proposed core structures, which have been designed optimally, is significantly better than that of the core structure St0 [10] at similar fibre parameters.

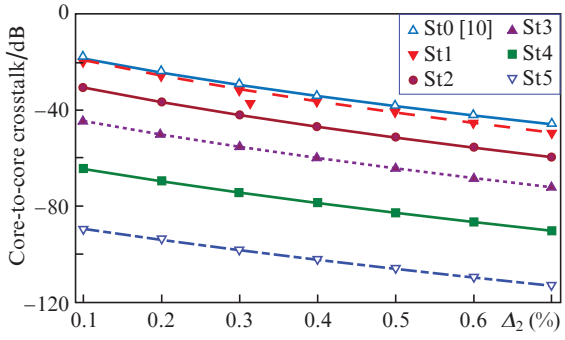

Figure 8. Dependences of the core-to-core crosstalk on the relative cladding/trench refractive index difference Δ_2 ar $\Lambda = 40$ μm and $W_t = 5$ μm.

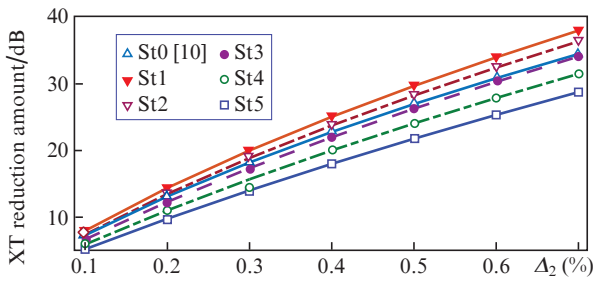

Figure 9. Dependences of the XT reduction amount on Δ_2 at $\Lambda = 40$ μm and $W_t = 5$ μm.

5.3. Crosstalk vs. trench width W_t

The trench width W_t plays a noteworthy role to achieve the lower XT level in MCF. The variations in the trench width and its impact on the XT level and its reduction amount are demonstrated in Figs 10 and 11, respectively. The XT reduction amount increases with increasing trench width W_t for all the considered core structures with the similar fibre parameters. One can clearly see from Fig. 10 that the XT level in MCF can be reduced remarkably to a low level by selecting the considerably higher values of Δ_1 and Δ_2. For example, the ultralow XT value, less than –100 dB per 100 km, can be achieved at a trench width of 3 and 6 μm, respectively, for St5 and St4 with $\Delta_2 = -0.70\%$. In addition, Fig. 10 clearly shows that St2 to St5 have substantially enhanced results in terms the ICXT levels in comparison with St0, while the XT performance of St1 is virtually similar to that of St0 [10].

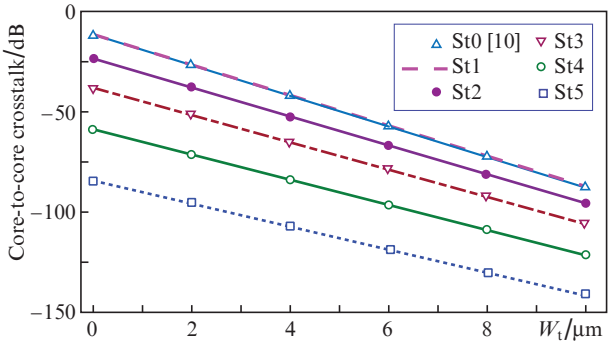

Figure 10. Core-to-core crosstalk vs. trench width W_t at $\Lambda = 40$ μm.

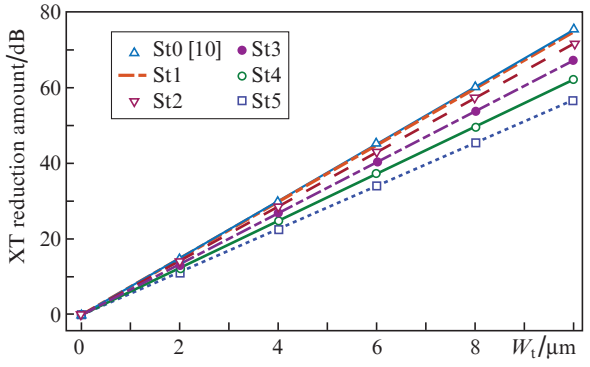

Figure 11. XT reduction amount vs. trench width W_t at $\Lambda = 40$ μm and $\lambda = 1550$ nm.

The difference in n_{eff} between the step-index core and the TA core is nearly of the order of 10^{-5} (see Table 1), which has a small effect on the variation of the cutoff wavelength. The theoretical un-cable cutoff wavelength is quite larger than the practical cable cutoff wavelength (it may be less than 1500 nm). Therefore, all the TA core structures are operated on the fundamental (LP_{01}) mode under the cutoff wavelength of the first higher order (LP_{11}) mode.

The analysis and discussions in Sub-sections 5.1 – 5.3 are essentially based on the fibre design parameters. These parameters must be chosen very precisely before the fabrication process, and hence, this kind of analysis will be extremely helpful, so that significantly lower XT levels along with the suitable XT reduction amount can be achieved for the cores of the MCF under the single-mode propagation condition. The analysis presented below is mainly based on the fibre operational parameters, such as fibre bending radius, wavelength and transmission distance. Once the MCF is fabricated, it is not possible to alter any fibre design parameters and, therefore, one can only study the impact of fibre operational parameters on the XT behaviour. Moreover, in Section 6 we ascertain which core structure is more preferable for short reach applications and for long distance optical communication, on the basis of performance in terms of crosstalk, dispersion and mode effective area.

5.4. Crosstalk vs. bending

The results of studying fibre bending on crosstalk behaviour are demonstrated in Figs 12 and 13 for trench depths of –0.70% and –1.40%, respectively, for all the proposed core structures. The XT deteriorates slowly with increasing bending radius of fibre. The improvements in the XT level is observed at a trench depth of –1.40% (see Sub-section 5.2). One can see that for a fibre bending radius of 140 mm, St3 to St5 have ultralow XT levels, less than –70 dB, which is mainly due to strong mode confinement and, hence, less coupling between the adjacent cores because high Δ_1 values and low core radii x_1 have been chosen for these structures.

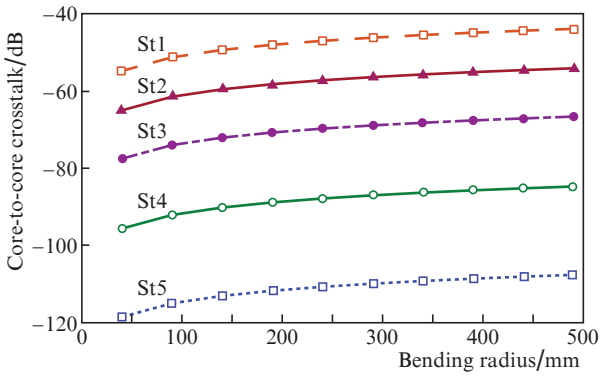

Figure 12. Core-to core crosstalk vs. fibre bending radius at $\Delta_2 = -0.70\%$ and $\Lambda = 40$ μm.

5.5. Crosstalk vs. wavelength

The analysis of the wavelength dependent XT is very important from the propagation point of view, especially in wave-

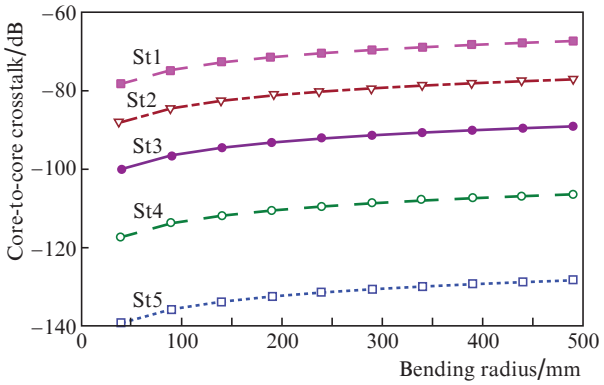

Figure 13. Core-to core crosstalk vs. fibre bending radius at Δ_2 = –1.40% and Λ = 40 μm.

length division multiplexing based optical systems and networks [22]. The analysis of the wavelength dependent XT relied on a wide range of operational wavelength, from 1530 nm to 1620 nm, as the attenuation loss over this range of wavelength does not exceed 0.2 dB km^{-1} [20]. In the course of the analysis of the simulation results we have found that the real part of n_{eff} decreases insignificantly with increasing wavelength (Fig. 14). The wavelength dependence of the XT performance for all the respective core structures is depicted in Figs 15 and 16 for trench depths Δ_2 = –0.70% and –1.40%, respectively. Again, for a wide range of wavelengths, the crosstalk is suppressed at a deeper trench depth (Fig. 16). A decrease in n_{eff} results in deterioration of MCF crosstalk performance, as depicted in Figs 15 and 16.

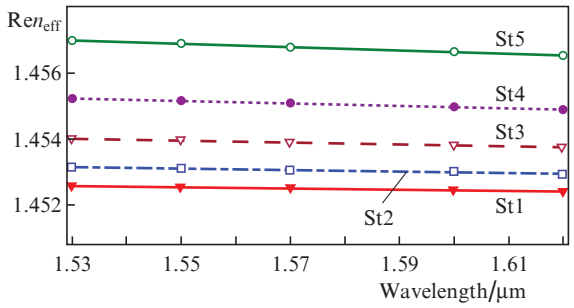

Figure 14. Dependences of Ren_{eff} on the wavelength for five different core structures.

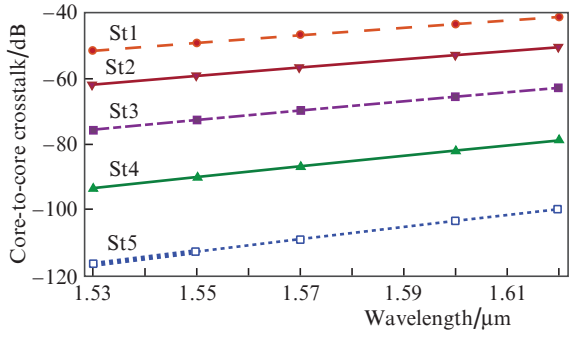

Figure 15. Core-to-core crosstalk vs. wavelength at Δ_2 = –0.70% and Λ = 40 μm.

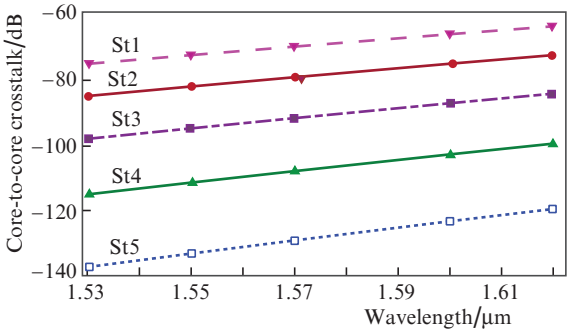

Figure 16. Core-to-core crosstalk vs. wavelength at Δ_2 = –1.40% and Λ = 40 μm.

5.6. Crosstalk vs. fibre length

For long-haul high-capacity communication, optical fibre cables are more preferable than metal wire cables. As demonstrated in Eqn (6), the crosstalk in MCF is directly dependent on the fibre length. The results of calculating the crosstalk performance with respect to a transmission distance up to 10000 km [5, 9] for all the five proposed core structures with fundamental (LP_{01}) mode propagation are demonstrated in Figs 17 and 18 for the trench depths Δ_2 = –0.70% and –1.40%. Here, the operating wavelength, core pitch, and fibre bending radius are assumed equal to 1550 nm, 40 μm and 140 mm, respectively. The FEM-based semi-analytical results show that the core-to-core crosstalk level reaches 10 dB with a tenfold increase in distance for all the respective five different core structures. For the transmission length of 100 Km, the ultralow crosstalk performance (no more than –70 dB) can be achieved with St3 to St5.

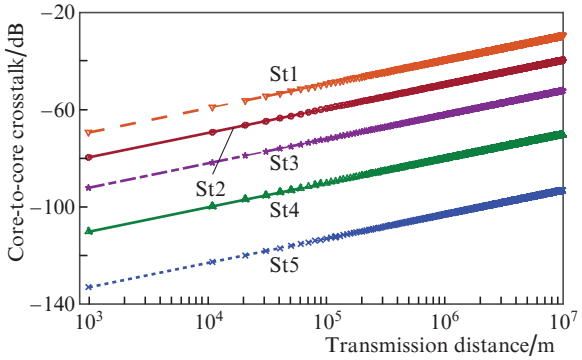

Figure 17. Core-to-core crosstalk vs. fibre length at Δ_2 = –0.70% and Λ = 40 μm.

6. Discussion of results

The worst crosstalk in a particular core can be estimated by taking into account the influence of all its neighbouring cores. The mean ICXT power level with multiple interfering adjacent cores with an equal core pitch is 10lgN_i (dB) higher than the one interfering core; here N_i is the number of interfering cores. In a seven-core MCF structure having a hexagonal close-packing (HCP) arrangement, the central and outer cores are interfered by 6 and 3 adjacent cores respectively,

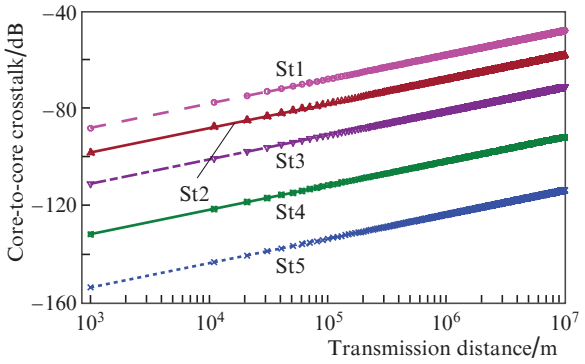

Figure 18. Core-to-core crosstalk vs. fibre length at $\Delta_2 = -1.40\%$ and $\Lambda = 40$ μm.

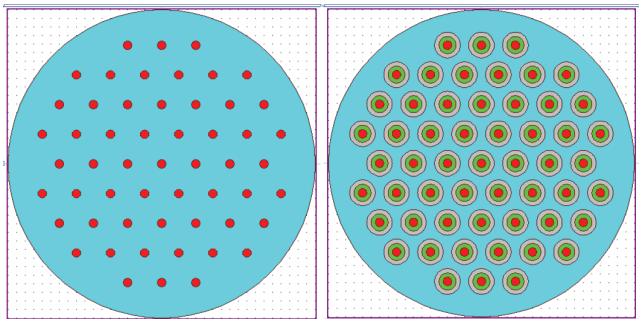

Figure 19. 55-core MCF with (left) a step-index core and (right) a TA-core.

which results in a corresponding increase in the mean XT value nearly by 7.8 dB and 4.8 dB in comparison to the case of only one interfering core.

Table 2 presents the ICXT level and its ΔXT for a step-index core and a TA core for all the five core structures at fixed fibre parameters, such as, $R_b = 140$ mm, $\lambda = 1550$ nm, $\Lambda = 40$ μm, $W_t = 5$ μm and $L = 100$ km. One can see that the crosstalk level improves significantly from St1 to St5, mainly due to a corresponding increase in Δ_1 and a decrease in x_1. The ultralow crosstalk (less than −100 dB per 100 km) performance can be achieved with St4 and St5 for the LP_{01} mode propagation in a seven-core MCF structure, which is a remarkably better result than that reported in [5, 13, 17]. Simultaneously, St4 and St5 have a low mode effective area, which is unsuitable for telecom services; therefore, these structure can be used for short reach applications like, optical interconnects [30], MCF sensors, etc. Structures St2 and St3 are quite acceptable for long-haul telecom communications, because of a low core-to-core crosstalk (less than −30 dB per 100 km) and effective mode area (nearly 60 to 90 μm^2), which follows the standards used in telecom services.

Moreover, for enhancing the data transmission capacity of a fibre with a large number of cores, the cladding diameter (CD) is to be large [16, 21], which poses challenges during the bending of fibre [6, 18, 19]. The 55-core MCF structure having the HCP lattice arrangement (Fig. 19) can be implemented with the cladding diameter CD = 302 μm, while keeping the core pitch $\Lambda = 32$ μm with CT = 35 μm, as obtained from the equation CD = $7\Lambda/\cos 15° + (2CT)$ μm.

The implementation of a 55-core MCF is possible with the proposed St5 with a normal step-index core for a target ICXT value of less than −30 dB per 100 km. This kind of the core structure design can reduce the design complexity by using a step-index profile instead of a TA core profile. It has been numerically estimated that St5 with a step-index core has a crosstalk level of −42 dB, which is better than the TA core structure based on St0 [10], where the XT level reaches nearly −20 dB with a trench depth of −0.70% and of −41 dB with a trench depth of −1.40%. The analysis also shows that the 55-core MCF can be anticipated with all the proposed structures with the TA core profile, where the worst XT is expected to be below −38 dB per 100 km. Nevetheless, the TA technique is a remarkable approach for crosstalk suppression in MCF, especially with lower number of cores, such as, 7 cores, 12 cores, etc. At the same time, to achieve the high information transmission capacity, the MCF with a larger number of cores is preferable, which complicates the design, particularly as in the case of TA MCF. Therefore, St4 and St5, with the step-index profile and single-mode propagation are more effective to reduce the design complexity and cost in comparison with the TA-based MCF designs as reported in [6, 10].

7. Conclusions

To achieve the ultralow crosstalk performance of MCF, we have proposed optimal designs of five different core structures with a core diameter from 6 to 10 μm and a corresponding relative core/cladding refractive index difference Δ_1 for single-mode propagation with a cutoff wavelength of nearly 1520 nm. The crosstalk has been estimated by using the semi-analytical method for a seven-core homogeneous trench-assisted multicore fibre. The crosstalk performance and its reduction amount (in dB) with respect to variations in several fibre design parameters, such as, relative core/cladding refractive index difference Δ_1, trench depth Δ_2 and trench width have been examined. The simulation results have shown that the crosstalk level and its suppression are significantly reliant on these parameters. The ultralow crosstalk levels can be achieved by optimally choosing the higher values of Δ_1 and Δ_2 with significantly smaller core radii. Moreover, the influence of some fibre operational parameters, such as fibre bending

Table 2. Crosstalk level and XT reduction amount ΔXT.

Structure	XT without a trench/dB	Trench, $\Delta_2 = -0.70\%$		Trench, $\Delta_2 = -1.40\%$	
		XT/dB	ΔXT/dB	XT/dB	ΔXT/dB
St0 [10]	−11.49	−45.91	34.42	−67.04	55.55
St1	−11.44	−49.37	37.94	−72.79	61.35
St2	−23.48	−59.58	36.01	−82.57	59.08
St3	−38.06	−72.08	34.02	−94.55	56.49
St4	−58.75	−90.18	31.43	−111.88	53.13
St5	−84.36	−113.05	28.69	−133.81	49.45

radius, operating wavelength and fibre length, on the crosstalk behaviour have also been demonstarted for the fundamental (LP_{01}) mode propagation. For each of the above fibre parameters, the crosstalk performance of the all the five MCF core structures have also been compared with St0 [10]. We have found that the proposed core structures have significantly enhanced crosstalk performance in comparison to St0 [10]. For all the proposed core structures, the simulation results have demonstrated significantly lower dispersion characteristics (approximately -6 ps nm^{-1} km^{-1} at 1550 nm). The ultralow crosstalk (less than -100 dB per 100 km) can be realised through the proposed core structures, St4 and St5, mainly due to the suitable selection of Δ_1 and core radius. A 55-core MCF has been designed with a step-index profile using the proposed structure St5 with a cladding diameter of 302 μm to avoid the fibre failure probability during the bending of fibre and to reduce the design complexity in comparison to trench-assisted cores. Structures St2 and St3 (having optimal core radii of 4.5 and 4 μm and $\Delta_1 \approx 0.4\%$ and 0.5%, respectively) are quite acceptable for long-haul telecom transmissions, because of a low crosstalk (less than -30 dB per 100 km) and a substantial effective mode area (from 60 to 90 μm^2), which comlies with the standards for telecom services. The core radius smaller than 4 μm, with its optimal Δ_1 value, complies with the ITU-T G.653 standards. It has a slightly lower effective area than the system used in ITU-T G.652 standards for telecom services. It does not practically degrade the single channel system; on the contrary, it may limit the capability of space division multiplexing systems. This kind of analysis can be highly beneficial for designing and characterising multicore fibres with an ultralow crosstalk, low dispersion and acceptable mode effective area before the fabrication process.

Acknowledgements. This research work is part of Early Career Research Award project (ECR/2017/000735) sponsored by Science and Engineering Research Board, Department of Science and Technology, Government of India. The authors gratefully acknowledge the National Institute of Technology Patna, India, for immense support.

References

1. Desurvire E.B. *J. Lightwave Technol*., **24** (12), 4697 (2006).
2. Essiambre R.J., Ryf R., et al. *IEEE Photonics J*., **5** (2), 0701307 (2013).
3. Richardson D.J., Fini J.M., et al. *Nat. Photonics*, **7**, 354 (2013).
4. Puttnam B.J., Luís R.S., et al., in *Proc. Europ. Conf. Netw. Opt. Comm*. (Portugal, 2016) pp 1–3.
5. Hayashi T., Taru T., et al. *Opt. Express*, **19** (17), 16576 (2011).
6. Saitoh K., Matsuo S. *J. Lightwave Technol*., **34** (1), 55 (2016).
7. Yao B., Ohsono K., et al., in *Proc. Opt. Fib. Comm. Conf. Exp., Nat. Fiber Opt. Eng. Conf*. (Los Angeles, USA, 2012) pp 1–3.
8. Ye F., Tu J., et al. *Opt. Express*, **22** (19), 23007 (2014).
9. Kumar D., Ranjan R. *Opt. Fib. Techn*., **41**, 95 (2018).
10. Ye F., Tu J., et al. *J. Lightwave Technol*., **34** (18), 4406 (2016).
11. Fini J.M., Zhu B., et al. *Opt. Express*, **18** (14), 15122 (2010).
12. Koshiba M., Saitoh K., et al. *Opt. Express*, **19** (26), B102 (2011).
13. Saitoh K., Koshiba M., et al. *IEEE Photonics Techn. Lett*., **24** (21), 1898 (2012).
14. Kumar D., Ranjan R., in *Proc. IEEE TENCON Conf. 2017* (Malaysia, 2017) pp 2405–2408.
15. Xia C., Bai N., et al. *Opt. Express*, **19** (17), 16653 (2011).
16. Matsuo S., Takenaga K., et al. *Opt. Lett*., **36** (23), 4626 (2011).
17. Hayashi T., Taru T., et al. *J. Lightwave Technol*., **30** (4), 583 (2012).
18. Goto Y., Nakajima K., et al. *J. Lightwave Technol*., **33** (23), 4942 (2015).
19. Sasaki Y., Takenaga K., et al. *Opt. Fib. Techn*., **35**, 19 (2017).
20. Hayashi T., Tamura Y., et al. *J. Lightwave Technol*., **35** (3), 450 (2017).
21. Sakaguchi J., Klaus W., et al. *J. Lightwave Technol*., **34** (1), 93 (2016).
22. Ye F., Tu J., et al. *IEEE Photonics Techn. Lett*., **28** (1), 27 (2016).
23. Jing Gao, Xia Zhang, Lei Shi, Weipeng Shi, Yongqing Huang, Xiaomin Ren. https://doi.org/10.1364/ACP.2011.83072O.
24. Aozasa S., Tsujikawa K., et al., in *Proc. Europ. Conf. Opt. Comm*. (Rome, Italy, 2018).
25. Elkin N.N., Napartovich A.P., et al. *Quantum Electron*., **32** (3), 264 (2002) [*Kvantovaya Elektron*., **32** (3), 264 (2002)].
26. Vysotskii D.V., Elkin N.N., et al. *Quantum Electron*., **32** (3), 271 (2002) [*Kvantovaya Elektron*., **32** (3), 271 (2002)].
27. Egorova O.N., Astapovich M.S., et al. *Quantum Electron*., **46** (3), 262 (2016) [*Kvantovaya Elektron*., **46** (3), 262 (2016)].
28. Egorova O.N., Astapovich M.S., et al. *Quantum Electron*., **46** (12), 1134 (2016) [*Kvantovaya Elektron*., **46** (12), 1134 (2016)].
29. Dianov E.M., Semjonov S.L., et al. *Quantum Electron*., **46** (1), 1 (2016) [*Kvantovaya Elektron*., **46** (1), 1 (2016)].
30. Hayashi T., Nakanishi T., et al. *J. Lightwave Technol*., **34** (1), 85 (2016).
31. Wolf A.A., Dostovalov A.V., et al. *Quantum Electron*., **48** (12), 1128 (2018) [*Kvantovaya Elektron*., **48** (12), 1128 (2018)].
32. Chekhovskoy I.S., Sorokina M.A., et al. *Quantum Electron*., **47** (12), 1150 (2017) [*Kvantovaya Elektron*., **47** (12), 1150 (2017)].
33. Kalinin N.A., Andrianov A.V., et al. *Quantum Electron*., **48** (4), 384 (2018) [*Kvantovaya Elektron*., **48** (4), 384 (2018)].
34. Kumar D., Ranjan R. *Opt. Eng*., **58** (5), 056109 (2019).
35. Okamoto K. *Fundamentals of Optical Waveguides* (San Diego, USA: Acad. Press, 2006) pp 183–187.